



Development and Characterization of Lignin Microparticles for Physical and Antioxidant Enhancement of Biodegradable Polymers

Raissa Alvarenga Carvalho Gomide¹ · Ana Carolina Salgado de Oliveira¹ · Danielle Aparecida Caetano Rodrigues¹ · Cassiano Rodrigues de Oliveira² · Odílio Benedito Garrido de Assis³ · Marali Vilela Dias¹ · Soraia Vilela Borges¹

Published online: 2 March 2020

© Springer Science+Business Media, LLC, part of Springer Nature 2020

Abstract

As the largest aromatic polymer of natural origin, lignin arouses the interest of researchers and industries worldwide. Its three-dimensional polymeric aromatic structure, besides being complex, varies depending on its botanical origin and extraction process, which makes its use as a raw material difficult. Currently, the main destination for lignin is burning for energy production. This study presents the characterization of lignin and lignin microparticles after processing by ultrasonic irradiation. Analyzes were performed to verify the dimensional, morphological and antioxidant characteristics of the particles as well as changes in their structure after sonication. A sample of eucalyptus wood lignin isolated from kraft black liquor was used and the modifications were analyzed by X-ray diffraction analysis, zeta potential, FTIR spectroscopy, particle size, scanning electron microscopy, TGA thermogravimetric analysis, phenolic compounds total by Folin–Ciocalteu and antioxidant analysis by DPPH. The results demonstrate that there was no change in the chemical structure of lignin with the application of ultrasonic radiation, but the reduction in particle size was able to reduce zeta potential with a lower probability of agglomeration between them, and consequent greater stabilization in solution. Also, the ultrasound treatment was able to increase the thermal stability of the lignin microparticle with a decrease of the mass loss rate with the time. The reduction in particle size was also able to expose a larger number of phenolic compounds and thereby increase the total phenolic content and lignin antioxidant activity making the lignin microparticle a promising material to study and application on food-active biodegradable polymers.

Keywords Microlignin · Packaging · Ultrasound · Microscopy · Thermal behavior

Introduction

Lignin, after cellulose, is the second most abundant component of wood, thus it is widely found in nature and is produced at a rate of 70 million tons per annum. It is a natural polymer compound with a phenylpropane structure. The abundance and potential for use in various sectors, such as fuels, biocides, chemicals, additives for paper and concrete, dispersants, cosmetics, paints, among others, have led to

an increase in the academic research and industry interests [1–8].

The primary precursors for lignin synthesis are hydroxycinnamic alcohols (monolignols), including coniferyl alcohol and synaphyl alcohol, with small amounts of ρ -coumaryl alcohol, joined by aromatic and aliphatic bonds and also by non-aromatic C–C bonds. Lignin exhibits a complex structure, containing cross-linked phenolic polymers and numerous functional groups such as aliphatic and phenolic hydroxyls and methoxy groups [9, 7, 10]. These functional groups affect the chemical and reactivity properties of lignin, thus determining its characteristics. Moreover, it is characterized as a highly branched amorphous phenolic compound, and its structure is considerably variable depending on the botanical origin, harvest period, and extraction process [11].

Recently, lignin micro- and nanoparticles have gained interest from researchers due to the improvement of their properties when compared to those of standard lignin, with

✉ Ana Carolina Salgado de Oliveira
anacarlengalimentos@gmail.com

¹ Food Science Department, Federal University of Lavras, Lavras, MG 37200-900, Brazil

² Institute of Exact and Technological Sciences, Federal University of Viçosa, Rio Paranaíba, MG 38810-000, Brazil

³ Embrapa Instrumentação, São Carlos, SP 13560-970, Brazil

several studies reported in the literature such as entrapping and encapsulation of pesticides, drugs, enzymes, sunscreen, surfactant, mechanical reinforcement material, and antioxidant activity of polymers [12, 13].

The use of biodegradable materials for film and packaging production has also been extensively studied, mainly aiming at reducing the environmental impact caused by the improper disposal of plastic packaging and as an alternative to the use of petroleum, a non-renewable source [14, 15]. Thus, the use of lignin at a micro or nanoscale may be an interesting alternative, once it has a biodegradable structure, and can be obtained as a co-product of the cellulose industry. When used in the production of films, these structures have a positive effect on the increase in UV barrier, besides the mechanical, thermal, antimicrobial, and antioxidant properties and the biocide effect in packaging materials [16–18].

Several methods of production of lignin micro- and nanoparticles have been reported in the literature, such as solvent or pH shifting, polymerization, ice-segregation, aerosol processing, mechanical processing, among others [1]. Mechanical processing is a simple method of producing lignin microparticles (LMP) and can be done using ultrasound. During the process, the occurrence of breakages and chemical reactions in the lignin structure is strongly related to the cavitation phenomenon, and in the case of polymers, ultrasound leads to the formation of homolytic breakage of chains, yielding a pair of radicals or polymerization with the formation of lignin monomers [19].

Therefore, this study aims to produce and characterize lignin microparticles (LMP) for later application as a biopolymer enhancement material. The LMP were produced by mechanical modification with ultrasound using the kraft black liquor technique. Then, the LMP were characterized for X-ray diffraction, zeta potential, Fourier transform infrared (FTIR) spectroscopy, particle size, scanning electron microscopy (SEM), thermogravimetric analysis (TGA), determination of phenolic compounds by Folin-Ciocalteu reagent, and the antioxidant potential by the DPPH free radical sequestration method.

Material and Methods

Materials

Lignin isolated from black kraft liquor was kindly donated by the Laboratory of Bioactive Products and Technological Solutions at Federal University of Viçosa (Rio Paranaíba Campus).

Synthesis of Lignin Microparticles

An aqueous suspension of lignin (0.7%, w/v) was used. The suspension was sonicated for 60 min, resulting in a stable microdispersion, which was dried under mild conditions (60 °C /24 h) before characterization. A sonicator (Sonifier Cell Disruptor Branson model 450D, Manchester, UK) was used at a frequency of 20 KHz and 400 W [19].

Characterization of the Particles

X-Ray Powder Diffraction (XRD)

The X-ray powder diffraction was performed in an XRD-6000 (Shimadzu) diffractometer with Cu- α 1 filter radiation ($\lambda = 1.5406 \text{ \AA}$), operating at 30 kV and 30 mA. The samples were fixed in aluminum support and analyzed at a scanning rate of 4°/min, with 2θ ranging from 5° to 70° at room temperature. The curves were analyzed using the software Origin® 9.0.

Zeta Potential

Zeta potential is a measure of the electrical charge of the material, from the interaction between a suspended colloidal solid material and a given liquid, using a Zetasizer Analyzer (Nano ZS ZEN 36000 - Malvern Instruments). The results of zeta potential were expressed in mV, and an average of 5 readings was performed for data analysis.

FTIR Analysis

Fourier transform infrared (FTIR) spectroscopy was performed using an FTS 3000 Excalibur Digilab (United States) spectrometer equipped with ATR detector, 4000–400 cm^{-1} spectral range, 64 scans, and 4 cm^{-1} resolution.

Particle Size

The particle size distribution of the samples was performed using the Zetasizer Analyzer (Nano ZS ZEN 36000 - Malvern Instruments). The equipment allows the determination of the particle size of the samples by the dynamic light scattering technique.

Scanning Electron Microscopy

The samples were mounted on aluminum stubs using double-coated carbon, gold-coated (SCD 050) and observed

on the Scanning Electron Microscope (LEO Evo 40) in the Electron Microscopy and Ultrastructural Analysis Laboratory.

Thermogravimetric Analysis

The thermal stability and degradation profile of the samples were determined by thermogravimetric analysis (TGA) in DTG60H-SHIMADZU apparatus (Shimadzu Corporation, Kyoto, Japan). The analysis was performed under a nitrogen atmosphere with a flow rate of 50 mL/min, heating from 25 to 800 °C, at a ratio of 10 °C/min, using 5 mg of sample.

Antioxidant Behavior

The antioxidant behavior of samples was evaluated according to the methodology described in previous work [20]. The total phenolics compounds (TPC) was determined spectrophotometrically by the Folin-Ciocalteu method. Briefly, a 0.2 mL aliquot of the extract was thoroughly mixed with 0.8 mL of 0.2 N Folin-Ciocalteu reagent and allowed to stand for 20 min in the dark. Then, 1 mL of 8.5% (w/v) sodium carbonate was added to the mixture and mixed gently. After a 30-min incubation, the mixture was centrifuged at 12,000×g rpm for 10 min. The supernatant was measured spectrophotometrically at 760 nm. A standard gallic acid solution was used for the construction of a calibration curve. TPC was calculated from the calibration curve, and the results were expressed as mg gallic acid equivalents (GAE)/g.

The radical scavenging activity (RSA) of lignin, lignin microparticles (MPL), and butylated hydroxytoluene (BHT synthetic antioxidant used as a reference) were determined by spectroscopy at 517 nm, measuring the reduction of the free radical 2,2-diphenyl-1-picrylhydrazyl (DPPH) (Sigma-Aldrich) by the antioxidant compound. The assay was performed by adding lignin aqueous solution in 2 mL DPPH solution in methanol (25 mg/L) to give a final lignin concentration of 30, 50, and 100 mg/L. After 30 min of reaction, the absorption was measured at 517 nm using a Bel SPECTRO S-2000 spectrophotometer (Monza, Italy). The antioxidant activity of the samples was expressed as follows:

$$(\text{RSA}\%) = (A_{\text{control}} - A_{\text{sample}}/A_{\text{control}}) \times 100$$

where A_{control} corresponds to the absorbance values of the control (methanol) at time zero and A_{sample} corresponds to the absorbance values of the samples at different reading times.

Statistical Analysis

The total phenolics compounds and antioxidant activity by DPPH were analysed using Statistica software (ver. 8, Stat

Table 1 Location of the maximum peak for lignin and LMP in XRD patterns and mean size of the ordered domain from Gaussian method

Sample	Fitting method	2θ (°)	R ²	FWHM ^a	Mean size of the ordered domain (nm)
Lignin	Pseudo-Vigot	20.26	0.94798	14.21961	0.59
MPL	Pseudo-Vigot	22.94	0.93344	13.91517	0.60

^aFWHM is obtained via Gaussian regression parameters set

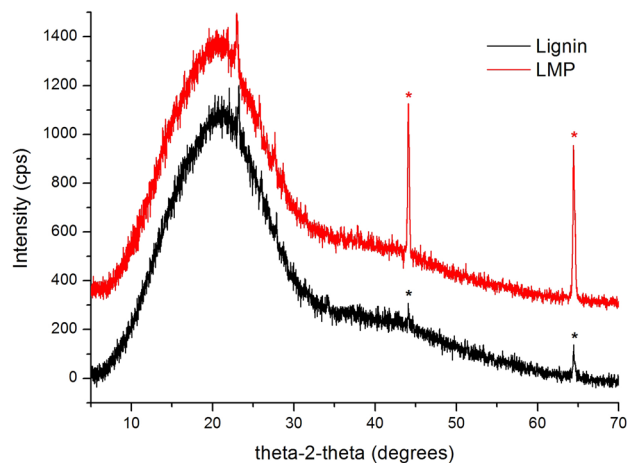


Fig. 1 XRD patterns of lignin and lignin microparticle (LMP). *Peaks corresponding to the aluminum sample holder

Soft Inc., Tulsa, USA). The analysis of variance test was used and the treatment means were compared by Tukey test.

Results and Discussion

X-Ray Powder Diffraction (XRD)

X-ray powder diffraction analysis was performed to study the morphology of lignin and LMP in more detail. For both the lignin and LMP samples, the diffractograms showed a wide area under the curve, which confirms the amorphous characteristic of both samples (Fig. 1). The maximum 2θ values were 20.26 and 22.94 for lignin and LMP, respectively.

The mean size of the ordered domain influences the process of incorporation of controlled-release agents to lignin. In order to identify ordered domains, peak fitting was performed by Gaussian, Lorentzian, Pearson VII and Pseudo-Vigot models. The best model fitting for lignin and LMP was Pseudo-Vigot at both diffractograms. Goudarzi et al. [21] found an average peak for hardwood located at $21.2 \pm 0.15^\circ$ while Kubo and Kadla [22] reported the acid lignin from hardwood average peak at 22.7° . Differences in chemical structures of lignins, method of isolation and type of sources

may explain the variation observed above. The mean size of the ordered domains is usually estimated by Scherrer's equation: $d = B\lambda/\beta\cos\theta$, where d is the mean size of the ordered domains, B = dimensionless shape factor (value of 0.9 is used), λ = X-ray wavelength (0.154 nm for Cu $K\alpha$), and β = full width at half maximum (FWHM) [21]. Table 1 shows the results of the calculated mean size of the ordered domains ("d" in Scherrer's equation) for lignin and LMP.

Lignin and LMP present almost the same values for the mean size ordered domains. This prove that amorphous behavior can be observed in both materials, being independent of sonication treatment. Thus, the reach of micrometers dimensions on lignin particles after sonication may not change the chemical composition, neither the spatial structure.

Zeta Potential

Zeta potential analysis of colloidal suspensions provides an overview of the stability and organization of particles in the medium, as it evaluates the repulsive or attractive electrostatic forces between the particles. For smaller sized materials, such as the lignin microparticles, the more negative the zeta potential value, the greater the electrostatic repulsion between particles and the greater the stability of the suspension, due to the little formation of aggregates when applied to nanocomposites.

The mean zeta potential values of lignin and lignin microparticles were 0.056 and -40.0 mV, respectively. The results found for lignin, close to zero, indicate no surface charge, and therefore a tendency for particle agglomeration on a larger scale. For the lignin microparticles, the negative values indicate a repulsion characteristic of the lignin microparticles, with a lower probability of agglomeration between them, and consequent greater stabilization [23].

The negative zeta potential value found for the LMP sample can be partially explained by the presence of negative phenol group charges and the possible adsorption of hydroxyl ions on the hydrophobic part of the microparticle. Moreover, the charges found may be associated with other functional groups such as carboxyls and sulfonic groups, in which oxygen atoms would be negatively charged [23].

Yang et al. [13] found zeta potential values ranging from -21.3 to -32.9 mV for nanolignin samples produced from acid hydrolysis. Mattinen et al. [24] found similar zeta potential values to this study when analyzing lignin nanoparticles treated or not with enzymes for crosslinking and consequent improvement of their application in biomaterials. The values found by them ranged from -29 to -47 mV. They correlate the decrease in zeta potential values with the increase in lignin particle oxidation and the formation of new carboxylic acid groups. The authors also correlate the decrease in value with the increase of lignin nanoparticle stability in

aqueous solution. Shulga et al. [25] also found zeta potential values ranging from -51 to -19 for lignin particles from two different plant sources and at different pH values (3.5, 5.8 and 11.0). According to the study, alkaline pH lignin particles showed the best results for oil-in-water emulsion stability (with the most negative zeta potential values) due to the presence of negatively charged ionic groups such as hydroxyls, carboxyls and phenolics on the surface of lignin.

FTIR Analysis

The results of the FTIR analysis show the main lignin and lignin microparticle bonds in the range of 4000 – 400 cm^{-1} , which is an important tool for the characterization of the structure of these samples. All spectra are shown in Fig. 2.

In general, the abundance of peaks for both samples demonstrates the structural complexity of lignin and LMP, probably due to the variety of vibrational modes of chemical bonds present in the polymer structures. In addition, the similarity between the spectra indicates small chemical changes between the samples, confirming the XRD results.

For both samples, the peaks at 2900 cm^{-1} correspond to the vibration of the C–H bond in methyl groups ($-\text{CH}_3$); the peaks at 1700 – 1660 cm^{-1} correspond to the C=O bond vibrations of carboxylic groups; the peaks at 1500 – 1600 cm^{-1} are characteristic of aromatic ring vibrations and C–H, O–H, C=O bonds; the peaks at 1460 cm^{-1} correspond to C–H bonds of methyl groups; the peaks at 1420 cm^{-1} correspond to aromatic ring vibrations; the peaks at 1370 cm^{-1} correspond to O–H bonds of phenolic and non-ether groups and syringyl units; the peaks at 1330 cm^{-1} correspond to vibrations in guaiacil groups; the peaks at 1160 – 1130 cm^{-1} refer to OH bonds of secondary alcohols; and finally the peaks at 1040 cm^{-1} characterize OH bonds of primary alcohols. In addition, LMP showed an increase in the absorption

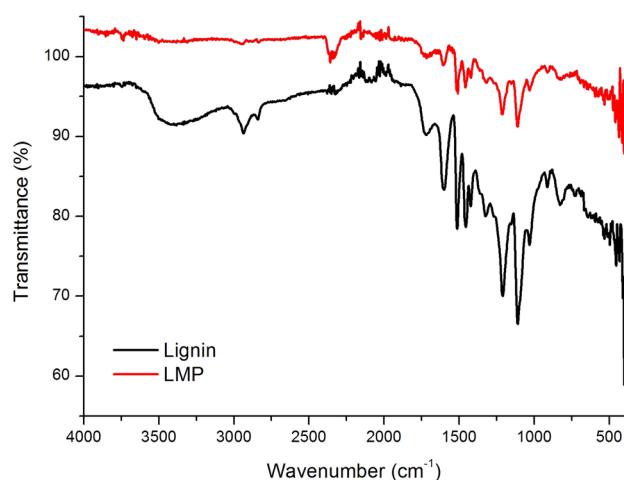


Fig. 2 FTIR spectra of lignin and lignin microparticle (LMP)

band at 1120 cm^{-1} , which is characteristic of condensed aromatic rings [21, 26].

For the lignin spectrum, a shoulder length at 860 cm^{-1} , characteristic of binding in arabinogalactan polysaccharides, was observed, which was not observed in LMP. A similar result was found by García et al. [27], who attributed the disappearance to the release of this type of hemicellulosic constituent from the main chain during sonication. The authors explain that the lateral hemicellulosic chains are the first to be affected after ultrasonic treatment, releasing mainly glucose and arabinose molecules from the lignin structure. The decrease in other bands intensity related to hemicellulosic constituent, i.e. xylose at 1030 cm^{-1} and glycosidic bonding at 895 cm^{-1} , were found to LMP sample being explained for the same reason.

When comparing both spectra, a decrease in peak intensity of MPL was observed when compared to lignin. This behavior may be due to the separation of hemicellulosic constituents from the lignin chain, leading to a decrease in peak intensity at $1160\text{--}1130\text{ cm}^{-1}$ and 1040 cm^{-1} . These groups correspond to the bonds between lignin units and monosaccharide units, as well as lignin-carbohydrate complexes, and the reduction of peak intensities is also related to the structural degradation of lignin and the hemicellulosic constituents, indicating that there was both removal of hemicelluloses and breakdown of the lignin molecule.

In the region corresponding to the O–H stretching absorption of the hydroxyl groups, from $3000\text{ to }3700\text{ cm}^{-1}$, higher peak intensity was observed for lignin when compared to LMP.

Particle Size Distribution

The results of particle size distribution showed the occurrence of a bimodal distribution with two mean peaks for the LMP at 605.5 nm (63.3%) and 475.8 nm (36.7%) while for lignin there was only an intense peak at 4849.0 nm (100%). It can be seen that the methodology was effective for the reduction of the lignin particle size.

According to Gilca et al. [19], the development of broken bonds and chemical reactions during the ultrasonic process is strongly related to the cavitation phenomenon. Cavitation is induced by high ultrasonic frequencies (16 KHz to 100 MHz) passing through the mass of the liquid. During the process, millions of air bubbles form in the liquid phase, at an adequate intensity allows the development of cavities. The collapse or inclusion of these cavities creates sites with high temperature and pressure in a short period, forming hot spots in the cold liquid. The transition state of these sites allows the first chemical reactions to occur during and after the microbubble collapse. In the presence of water and air, hydroxyl and superoxide radicals are formed. Furthermore, the radicals formed during the sonication process depend

on the number of cavities and radicals formed per cavity. In the case of polymers, the ultrasonic process treatment can lead to the formation of homolytic breakage of macromolecular chains, yielding a pair of radicals or polymerization of monomers with a consequent decrease in size.

As explained in item 3.3, during the ultrasonic radiation process there is a removal of hemicellulosic impurities from the lignin structure. Hemicelluloses are usually composite of the main chain of xylose units from which come shorter branches formed by glucose, arabinose and xylose units and the release of these monosaccharides during sonication occurs exactly from these side chains, with the proportion between them varying according to botanical origin and lignin extraction methods. Also, during periods of sonication longer than 30 min, degradation or transformation of these released polysaccharides may occur. Studies also indicate that after the treatment of lignin with ultrasonic radiation, there is a tendency to decrease its molecular weight, with most of the resulting components becoming smaller monomers or hemicellulosic chains [28].

Scanning Electron Microscopy

The micrographs of dried lignin and lignin microparticles are shown in Fig. 3 and confirm the results obtained by dynamic light scattering, i.e., a decrease in size after the ultrasonic treatment.

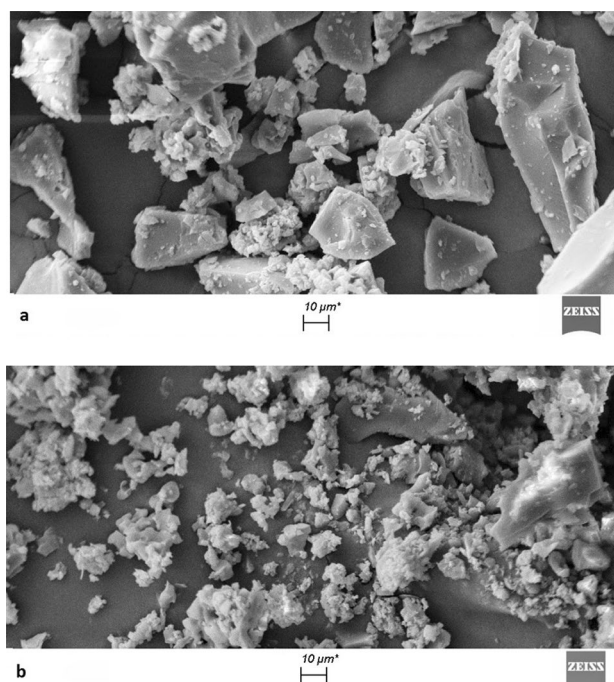


Fig. 3 Micrographs obtained by scanning electron microscopy of lignin (a) and lignin microparticles LMP (b) at $\times 1000$ magnification

The micrographs of lignin and LMP are in accordance with those reported in the literature. Meng et al. [29] found similar images for *kraft* lignin and characterized the sample by an irregular morphology. Lu et al. [11] found similar micrographs for lignin and relate the reduction of particle size with the increase in antioxidant activity related to the bigger surface contact area in the samples.

Thermogravimetric Analysis (TGA)

Different methods and temperatures can be used in the production of biodegradable polymers. Therefore, the study of the thermal properties of lignin and lignin microparticle was needed [30]. The thermal properties of the samples were investigated by TGA analysis, and Fig. 4 shows the TG and DTG thermograms of lignin and lignin microparticles. For both samples, a varied thermal decomposition was observed, characteristic of their complex structures.

In the range between 50 and 150 °C a first mass loss was observed for both samples. This phenomenon was associated to moisture release from the sample. A second degradation step was detected from approximately 150 to 300 °C and corresponded to the thermal decomposition of lignin-linked

hemicelluloses [28]. The non-irradiated lignin sample began to decompose at 181.0 °C and showed a maximum degradation peak at 338 °C. For the lignin microparticle (all data are not shown in Table 2) the onset of the degradation happened close to 193.0 °C and the maximum weight loss occurred at 715.2 °C. Many authors have related this behavior to the molecular weight of lignin [2]. Therefore, the thermal stability of the lignin microparticle was improved after ultrasonic irradiation.

Studies relate weight loss between 300 and 500 °C with thermal degradation of lignin. This behavior was observed for both samples and an increase of the mass loss rate with the time at the maximum degradation point of the lignin was

Table 2 Thermal behavior of lignin and LMP by the thermogravimetric analysis

Sample	T_i (°C)	T_{max} (°C)	T_f (°C)	(%) PM (T_i-T_f)	Res _{800 °C} (%)
Lignin	181.0	338.0	756.9	72.4	18.6
MPL	193.3	715.2	763.1	59.0	27.1

T_i initial degradation temperature, T_{max} maximum degradation temperature, T_f final degradation temperature, (%) PM ($T_i - T_f$) percentage of mass loss, Res_{800 °C} residue at 800 °C

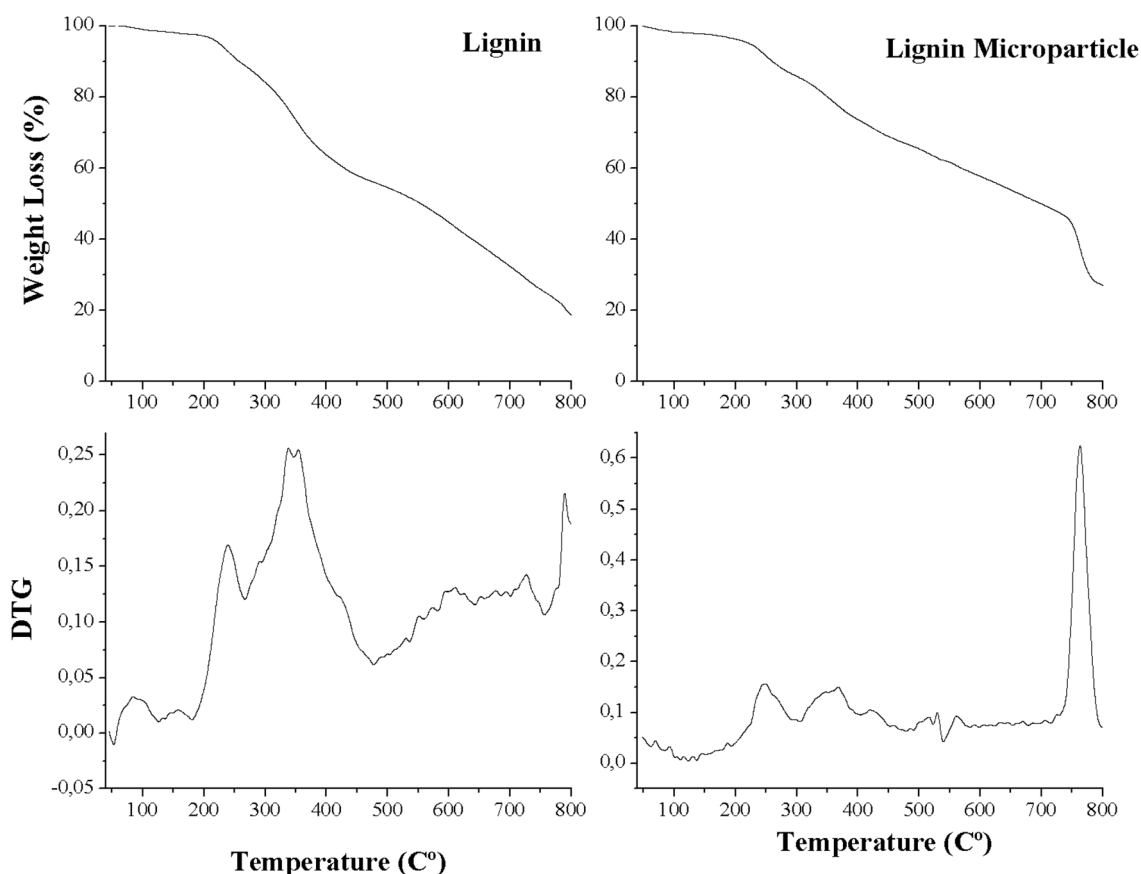


Fig. 4 TG and DTG thermograms of lignin and lignin microparticles

detected, being almost constant lignin microparticle. This fact, and the lowest degradation rate indicated a low content of hemicelluloses in lignin microparticle. These results are in agreement with those obtained by other authors [31, 28], indicating lower hemicellulosic impurities in lignin microparticle.

Finally, an abrupt weight loss above 700 °C was observed in both samples. Such degradation was previously ascribed to the cracking of the xylan backbone. In general the lignin final residue that remain after non oxidizing thermal degradation reaches values between 30 and 40%, which could be smaller when hemicellulosic contamination is detected. García et al. [27] found similar values for final residue of lignin after 60 min ultrasound treatment (30.7%) and relates this result to the higher purity of these samples. This fact can be related to the removal of hemicellulosic portions during ultrasound treatment, corroborating once more the results discussed above.

Antioxidant Behavior

Total phenolic content (TFC) of the analyzed lignin and LMP samples were $14.81\% \pm 0.02$ and $19.03\% \pm 0.03$, respectively, with statistically differ ($p < 0.05$). Lignin sample presented low TFC, which corroborated those reported in previous works [32].

TFC suffered an abrupt increase of 28% after 60 min of sonication. García et al. [27] also found the maximum amount of phenolics in sample isolated after 60 min of ultrasonic treatment and correlates with the decreased in hemicelluloses content. So, this fact was probably related to inorganic and hemicellulosic impurities release after ultrasonic treatment, which was likewise observed in the 3.4 and 3.5 items. In this way, the removal of these interfering compounds resulted in an improvement of TFC.

Oxygen-free radicals can be found naturally or derived from thermal processes or irradiation. The efficiency of free radical scavenging activity of an antioxidant compound depends on the hydrogen atoms exchange reactions and the stability of the radical resulting from the reaction. The antioxidant activity of lignin and lignin microparticles was investigated by the DPPH assay, as it is considered an available free radical and widely used to study the lignin antioxidant potential [33, 13].

Table 3 shows the DPPH antioxidant activity of lignin, lignin microparticles, and BHT (synthetic antioxidant) at different concentrations after 30 min of incubation. The results show a more intense antioxidant activity for LMP when compared to the conventional lignin. Absorption values at 517 nm decrease with increasing the concentration and antioxidant activity of the samples, reaching a sequestration activity close to 50% to 100 mg/L after 30 min of activity. The antioxidant activity of lignin is due to its high number

Table 3 DPPH free radical scavenging activity of different concentrations (mg/L) of lignin, lignin microparticle (LMP), and BHT in DPPH/methanol solution after 30 min of reaction

Sample	Concentration (mg/L)	Absorbance $\lambda = 517$ nm	RSA* (%)
Lignin	30	$1.001 \pm 0.002^{**}$	$7.91^a \pm 0.19$
	50	0.847 ± 0.021	$22.07^c \pm 1.93$
	100	0.679 ± 0.015	$37.53^e \pm 1.38$
MPL	30	0.888 ± 0.012	$18.30^b \pm 1.10$
	50	0.710 ± 0.026	$34.68^d \pm 2.39$
	100	0.567 ± 0.024	$47.83^f \pm 2.20$
BHT	30	0.859 ± 0.013	$20.97^b \pm 1.20$
	50	0.604 ± 0.029	$44.43^d \pm 2.67$
	100	0.462 ± 0.020	$57.49^g \pm 1.84$

*Averages observed in columns with the same letter do not statistically differ ($p < 0.05$)

**Standard deviation

of phenolic groups, which passes through a proton-coupled electron transfer mechanism. Some studies have shown that the greater antioxidant effect of lignin depends on several factors, including a high amount of phenolic groups with or without methoxyl groups, a low amount of aliphatic oxygen-containing groups (such as alcohols, ketones, and esters), low molecular weight, and a narrow polydispersity. During the sonication process, the molecular weight and polydispersity of lignin decreased, as also observed in other studies [19, 13, 27].

The higher antioxidant activity of LMP when compared to lignin may also be due to possible removal of inorganic materials and hemicellulosic impurities during sonication, exposing portions of lignin with antioxidant activity. In addition, other factors such as increased contact surface area due to the lower particle size of lignin may have contributed to a greater binding capacity of protons for the phenolic groups from LMP.

Conclusion

In the present work, ultrasound was applied in kraft lignin. XRD and FTIR confirmed the amorphous behavior and probable maintenance of chemical composition and spatial structure in samples. Zeta potential shows a repulsion characteristic of the lignin microparticles, with a lower probability of agglomeration between them, and consequent greater stabilization. Particle size and scanning electron microscopy confirm the efficiency of ultrasound in reduced diameter of particles and can be explained mainly due to inorganic and hemicellulosic impurities release after ultrasonic treatment. Antioxidant behavior was also improved and can be explained by the removal of these interfering compounds.

The thermal behavior analysis of the samples showed that the ultrasound treatment was able to increase the thermal stability of the lignin microparticle with a decrease in the mass-loss rate with the time. These results show the potential use of lignin microparticles obtained by ultrasound treatment as reinforcing the material and/or antioxidant to biodegradable polymers.

Acknowledgements Authors thank FAPEMIG (Research Support Foundation of the State of Minas Gerais), CNPq (National Council for Scientific and Technological Development) and CAPES (Coordination of Improvement of Higher Level Personnel) for financial support and scholarships. Authors would like to thank Laboratory of Electron Microscopy and Analysis of Ultrastructural (<http://www.prp.ufla.br/labs/microscopiaeletronica/>), of Federal University of Lavras (UFLA) for supplying equipment and technical support for experiments involving electron microscopy. Authors would like to thank Central of Analysis and Chemical Prospecting of UFLA for supplying equipment and technical support for experiments involving FTIR and TGA analyzes.

References

- Beisl S, Friedl A, Miltner A (2017) Lignin from micro-to nano-size: applications. *Int J Mol Sci* 18(11):2367
- Spiridon I, Poni P, Ghica G, Alley V (2018) Biological and pharmaceutical applications of lignin and its derivatives: a mini-review. *Cellul Chem Technol* 52(7–8):543–550
- Setälä H, Alakomi H-L, Paananen A, Szilvay GR, Kellock M, Lievonen M, Liljeström V, Hult E-L, Lintinen K, Österberg M, Kostiaainen M (2019) Lignin nanoparticles modified with tall oil fatty acid for cellulose functionalization. *Cellulose*. <https://doi.org/10.1007/s10570-019-02771-9>
- Zhang N, Tao P, Lu Y, Nie S (2019) Effect of lignin on the thermal stability of cellulose nanofibrils produced from bagasse pulp. *Cellulose* 26(13–14):7823–7835
- Shukla A, Sharma V, Basak S, Ali SW (2019) Sodium lignin sulfonate: a bio-macromolecule for making fire retardant cotton fabric. *Cellulose* 26(13–14):8191–8208
- Chen R, Abdelwahab MA, Misra M, Mohanty AK (2014) Biobased ternary blends of lignin, poly(lactic acid), and poly(butylene adipate-co-terephthalate): the effect of lignin heterogeneity on blend morphology and compatibility. *J Polym Environ* 22(4):439–448. <https://doi.org/10.1007/s10924-014-0704-5>
- Sathawong S, Sridach W, Techato K-a (2018) Recovery of Kraft lignin from OPEFB and using for lignin–agarose hydrogel. *J Polym Environ* 26(8):3307–3315. <https://doi.org/10.1007/s10924-018-1218-3>
- Panzarasa G, Osypova A, Ribera J, Schwarze FW, Quasso F, Consolati G (2018) Hybrid adsorbent materials obtained by the combination of poly(ethylene-alt-maleic anhydride) with lignin and lignosulfonate. *J Polym Environ* 26(11):4293–4302. <https://doi.org/10.1007/s10924-018-1299-z>
- Vanholme R, Demedts B, Morreel K, Ralph J, Boerjan W (2010) Lignin biosynthesis and structure. *Plant Physiol* 153(3):895–905. <https://doi.org/10.1104/pp.110.155119>
- Ramezani N, Sain M (2018) Thermal and physicochemical characterization of lignin extracted from wheat straw by organosolv process. *J Polym Environ* 26(7):3109–3116. <https://doi.org/10.1007/s10924-018-1199-2>
- Lu Q, Zhu M, Zu Y, Liu W, Yang L, Zhang Y, Zhao X, Zhang X, Zhang X, Li W (2012) Comparative antioxidant activity of nanoscale lignin prepared by a supercritical antisolvent (SAS) process with non-nanoscale lignin. *Food Chem* 135(1):63–67. <https://doi.org/10.1016/j.foodchem.2012.04.070>
- Sipponen MH, Lange H, Crestini C, Henn A, Österberg M (2019) Lignin for nano- and microscaled carrier systems: applications, trends, and challenges. *ChemSusChem* 12(10):2039–2054. <https://doi.org/10.1002/cssc.201900480>
- Yang W, Fortunati E, Gao D, Balestra GM, Giovanale G, He X, Torre L, Kenny JM, Puglia D (2018) Valorization of acid isolated high yield lignin nanoparticles as innovative antioxidant/antimicrobial organic materials. *ACS Sustain Chem Eng* 6(3):3502–3514. <https://doi.org/10.1021/acssuschemeng.7b03782>
- de Castro e Silva P, de Oliveira ACS, Pereira LAS, Valquíria M, Carvalho GR, Miranda KWE, Marconcini JM, Oliveira JE. Development of bionanocomposites of pectin and nanoemulsions of carnauba wax and neem oil pectin/carnauba wax/neem oil composites. *Polym Compos*. <https://doi.org/10.1002/pc.25416>
- Carvalho R, Oliveira A, Santos T, Dias M, Yoshida M, Borges S (2019) WPI and cellulose nanofibres bio-nanocomposites: effect of thyme essential oil on the morphological, mechanical, barrier and optical properties. *J Polym Environ*. <https://doi.org/10.1007/s10924-019-01598-6>
- Kovalcik A, Machovsky M, Kozakova Z, Koller M (2015) Designing packaging materials with viscoelastic and gas barrier properties by optimized processing of poly(3-hydroxybutyrate-co-3-hydroxyvalerate) with lignin. *React Funct Polym* 94:25–34. <https://doi.org/10.1016/j.reactfunctpolym.2015.07.001>
- Yang W, Fortunati E, Dominici F, Giovanale G, Mazzaglia A, Balestra GM, Kenny JM, Puglia D (2016) Synergic effect of cellulose and lignin nanostructures in PLA based systems for food antibacterial packaging. *Eur Polym J* 79:1–12. <https://doi.org/10.1016/j.eurpolymj.2016.04.003>
- Yang W, Owczarek JS, Fortunati E, Kozanecki M, Mazzaglia A, Balestra GM, Kenny JM, Torre L, Puglia D (2016) Antioxidant and antibacterial lignin nanoparticles in polyvinyl alcohol/chitosan films for active packaging. *Ind Crops Prod* 94:800–811. <https://doi.org/10.1016/j.indcrop.2016.09.061>
- Gilca IA, Popa VI, Crestini C (2015) Obtaining lignin nanoparticles by sonication. *Ultrason Sonochem* 23:369–375. <https://doi.org/10.1016/j.ultrsonch.2014.08.021>
- Juttuporn W, Thiengkaew P, Rodklongtan A, Rodprapakorn M, Chitprasert P (2018) Ultrasound-assisted extraction of antioxidant and antibacterial phenolic compounds from steam-exploded sugarcane bagasse. *Sugar Tech* 20(5):599–608
- Goudarzi A, Lin L-T, Ko FK (2014) X-ray diffraction analysis of kraft lignins and lignin-derived carbon nanofibers. *J Nanotechnol Eng Med* 5(2):021006
- Kubo S, Kadla JF (2005) Lignin-based carbon fibers: effect of synthetic polymer blending on fiber properties. *J Polym Environ* 13(2):97–105. <https://doi.org/10.1007/s10924-005-2941-0>
- Liu Z-H, Hao N, Shinde S, Pu Y, Kang X, Ragauskas AJ, Yuan JS (2019) Defining lignin nanoparticle properties through tailored lignin reactivity by sequential organosolv fragmentation approach (SOFA). *Green Chem* 21(2):245–260. <https://doi.org/10.1039/C8GC03290D>
- Mattinen M-L, Valle-Delgado JJ, Leskinen T, Anttila T, Riviere G, Sipponen M, Paananen A, Lintinen K, Kostiaainen M, Österberg M (2018) Enzymatically and chemically oxidized lignin nanoparticles for biomaterial applications. *Enzyme Microb Technol* 111:48–56. <https://doi.org/10.1016/j.enzmictec.2018.01.005>
- Shulga G, Livcha S, Neiberte B, Verovkins A, Vitolina S, Zhilinska E (2019) The effect of pH on the ability of different lignins to stabilize the oil-in-water emulsion. In: IOP conference series: materials science and engineering, vol 1. IOP Publishing, Bristol, p 012011
- Santos PSBD, Erdocia X, Gatto DA, Labidi J (2014) Characterisation of Kraft lignin separated by gradient acid precipitation.

- Ind Crops Prod 55:149–154. <https://doi.org/10.1016/j.indcrop.2014.01.023>
27. García A, Erdocia X, González Alriols M, Labidi J (2012) Effect of ultrasound treatment on the physicochemical properties of alkaline lignin. *Chem Eng Process* 62:150–158. <https://doi.org/10.1016/j.cep.2012.07.011>
 28. García A, Alriols MG, Llano-Ponte R, Labidi J (2011) Ultrasound-assisted fractionation of the lignocellulosic material. *Biores Technol* 102(10):6326–6330. <https://doi.org/10.1016/j.biortech.2011.02.045>
 29. Meng L-Y, Ma M-G, Ji X-X (2019) Preparation of lignin-based carbon materials and its application as a sorbent. *Materials* 12(7):1111
 30. Yuan T-Q, Sun S, Xu F, Sun R (2011) Isolation and physicochemical characterization of lignins from ultrasound irradiated fast-growing poplar wood. *BioResources* 6(1):414–433
 31. Yang B, Zhao M, Shi J, Yang N, Jiang Y (2008) Effect of ultrasonic treatment on the recovery and DPPH radical scavenging activity of polysaccharides from longan fruit pericarp. *Food Chem* 106(2):685–690. <https://doi.org/10.1016/j.foodchem.2007.06.031>
 32. García A, González Alriols M, Labidi J (2012) Evaluation of the effect of ultrasound on organosolv black liquor from olive tree pruning residues. *Biores Technol* 108:155–161. <https://doi.org/10.1016/j.biortech.2012.01.010>
 33. Domenek S, Louaifi A, Guinault A, Baumberger S (2013) Potential of lignins as antioxidant additive in active biodegradable packaging materials. *J Polym Environ* 21(3):692–701

Publisher's Note Springer Nature remains neutral with regard to jurisdictional claims in published maps and institutional affiliations.